

PHOTOGRAMMETRIC PROCESSING OF LOW ALTITUDE IMAGE SEQUENCES BY UNMANNED AIRSHIP

Yongjun Zhang

School of Remote Sensing and Information Engineering, Wuhan University, Wuhan, Hubei, 430079, P.R. China -
zhangyj@whu.edu.cn

Commission V

KEY WORDS: Image Sequence, Close Range Photogrammetry, Matching, Aerial Triangulation, Accuracy Analysis, Topographic Mapping

ABSTRACT:

Low altitude aerial image sequences have the advantages of high overlap, multi viewing and very high ground resolution. These kinds of images can be used in various applications that need high precision or fine texture. This paper mainly focuses on the photogrammetric processing of low altitude image sequences acquired by unmanned airship, which automatically flies according to the predefined flight routes under the controlment of autopilot system. The overlap and relative rotation parameters between two adjacent images are estimated by matching two images as a whole and then precisely determined by pyramid based image matching and relative orientation. The matched image points and ground control points are then used for aerial triangulation with collinearity equations. The aerial triangulated high resolution images can be used to obtain precise spatial information products, such as Digital Surface Model (DSM), Digital Ortho Map (DOM) large scale Digital Linear Graphic (DLG) and three-dimensional (3D) city model. Experimental results show that the developed remote sensing system is qualified for high overlap and high resolution stereo imagery acquisition. Moreover, the proposed approaches are effective for photogrammetric processing of low altitude image sequences, and have well potentials in large scale topographic mapping and precise 3D reconstruction areas.

1. INTRODUCTION

In photogrammetric applications, image acquisition is one of the most expensive steps. Using a flexible and efficient way to obtain aerial images has been the primary purpose of many photogrammetric researchers and communities.

As compared with film based camera, digital camera is advantageous for its ability of high forward overlap (e.g. 80%) image acquisition without increasing flight strips. In this case, every ground feature has at least 5 corresponding image features (Zhang, 2005a). High overlap image sequences are also advantageous for image matching and 3D reconstruction (Zhang, 2005b).

Along with the development of unmanned aerial vehicles, popularization of non-metric digital cameras and progress of photogrammetric technologies, low altitude images has been a hot spot in photogrammetric areas. Low altitude high resolution aerial images have well potentials in applications of large scale mapping, true orthophoto generation, archaeology and 3D city modeling. Now, the mostly used low altitude platforms for image data acquisition are helicopters (Zhang, 2005b), remote controlled model aircrafts (Nogami, 2002; Sun, 2003) or tethered balloons (Huang, 2003).

Although considerable results of photogrammetric processing of low altitude images have been achieved (Karras, 1999; Bitelli, 2004; Altan, 2004; Zhang, 2005b), the acquisition and photogrammetric processing of low altitude image sequences with unmanned platforms is still at an early stage.

The typical characteristic of images taken from low altitude platforms is that the predefined relationship between adjacent images cannot be guaranteed strictly. There are usually large

overlap variations and large rotation angles between adjacent images, and also large parallax discontinuities between features above the ground. So terrain continuity constraint that used by most traditional matching algorithms is invalid for low altitude images.

General strategy for photogrammetric processing of low altitude image sequences, composition of the developed low altitude remote sensing system and data acquisition for experiments are described in section 2. Afterwards, detailed approach for photogrammetric processing, including image matching, relative orientation and aerial triangulation are discussed. Experimental results of photogrammetric processing and digital photogrammetric product generation are given in section 4. Finally, conclusions are given and further work is highlighted.

2. GENERAL STRATEGY AND DATA ACQUISITION

2.1 General strategy

The photogrammetric processing of low altitude image sequences, such as image matching, relative orientation, aerial triangulation, DSM and DOM generation and large scale mapping are the content of the current work. The image sequences are automatically acquired by a low altitude remote sensing system based on unmanned airship. Firstly, the overlap and relative rotation parameters between two adjacent images are estimated by matching two images as a whole and then precisely determined by image matching and relative orientation process. Image matching is also constrained by epipolar line, which is determined by relative orientation parameters. The matched image points and ground control points are both used for aerial triangulation with collinearity equations. Orthoimage is rectified after DSM is generated by dense image matching

and forward intersection. Finally, the aerial triangulated high resolution images are also used for obtaining precise spatial information, such as building outlines and large scale mapping.

2.2 Low altitude remote sensing system with unmanned airship

With several years' research in corporation with another group, low altitude remote sensing system based on unmanned airship is developed. The unmanned airship automatically flies according to predefined flight routes under controlment of autopilot system. Hardware of the remote sensing system is composed of unmanned airship, autopilot system, task payload, wireless communication equipment, ground control station and optional GPS reference station, as shown in figure 1.

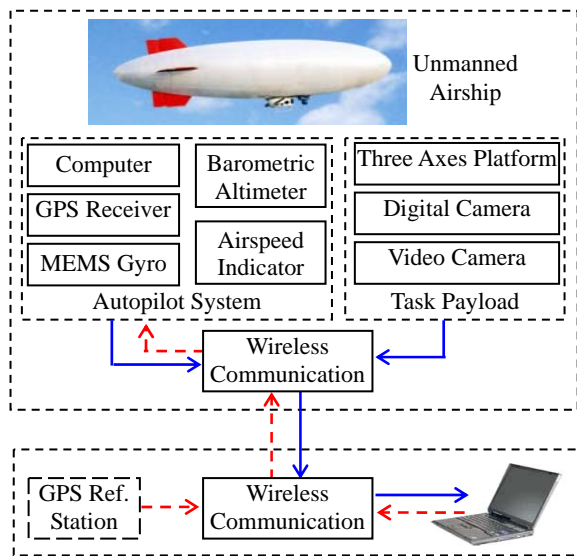


Figure 1. Hardware of the low altitude remote sensing system

The autopilot system is composed of computer, GPS receiver, MEMS gyroscope, barometric altimeter, airspeed indicator and flying control software. The autopilot system collects real time information such as position and speed of the unmanned airship and automatically controls the unmanned airship according to predefined flying routes. The task payload consists of digital camera, video camera and three axes stabilising platform on which the two cameras fixed on. The platform can automatically keep the predefined camera orientation against the swing or oscillation of unmanned airship. The dashed arrows in figure 1 indicate control signals and information transformation from the ground station to autopilot system by wireless communication equipment, while bold arrows indicate the information and data transformation (e.g. real time video) from the autopilot system and task payload to ground station.

Technical parameters of the low altitude remote sensing system are listed in the following: length of the airship is 13.2m, cruising speed is about 30~40km/h, maximum payload capacity is about 15kg, accuracy of flying tracks against the predefined routes is about 5m, posture maintaining accuracy of the three axes stabilising platform is about 3 degrees in roll and pitch and 5 degrees in yaw. The non-metric camera fixed on the platform is Kodak Pro SLR with 4500pixels*3000pixels image format and 0.008mm pixel size.

2.3 Data acquisition

The unmanned airship can automatically fly according to the predefined flight routes under controlment of autopilot system. Low altitude aerial image sequences are taken by the aforementioned non-metric digital camera. The camera is fixed on three axes stabilising platform, which can keep the camera orientation more stable than the airship itself while flying.

Low altitude image sequences for experiments are taken with the developed remote sensing system in Nov. 2007. Wind speed is about 7m/sec during image data acquisition. Ground coverage of the test area is about 700m*700m. The flying height of unmanned airship above the ground is about 150m. 24mm lens is mounted on the Kodak Pro SLR Camera. So ground coverage of each image is 150m*225m, and ground sample distance (GSD) of images is about 0.05m. Predefined distance between two exposure points is 28m, and distance between two strips is 50m, i.e. the forward overlap and side overlap is 80% and 75% respectively. Totally 299 images of 13 strips are taken with the unmanned airship. Figure 2 shows the planar position of camera center of all images. Caused by wind sensitivity characteristics and imperfection of the three axes platform, the maximum bias from exposure point to predefined flying strip is about 5m, height maintaining accuracy when compared with predefined flying height is better than 10m, orientation variations between adjacent images are about 5 degrees. Five typical stereo images of one strip are shown in figure 3. As can be seen, the overlap and camera orientation are stable and fitted with that of the predefined ones.

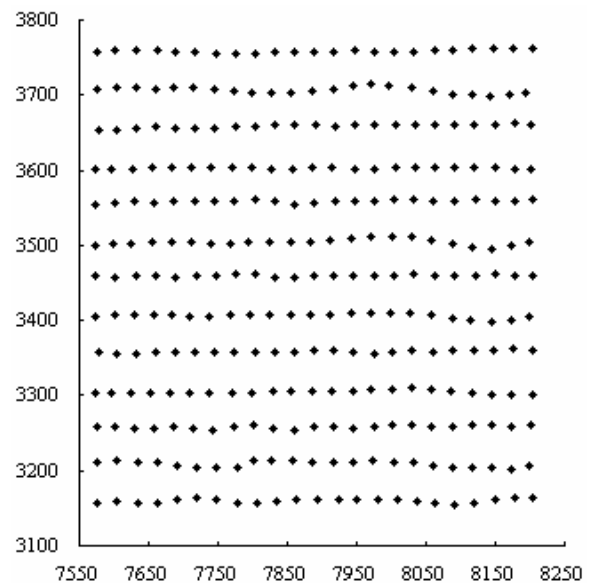


Figure 2. Planar position of exposure points



Figure 3. Stereo images taken by the remote sensing system

To fully evaluate the precision of image sequences acquired by the low altitude remote sensing system, totally 64 ground points

with white feature marks are measured by total station. The planar and height precision of these control points are all better than 0.015m. Figure 4 shows the distribution of ground feature points. The 33 triangular shaped points are used as control points, while the other 31 square shaped points are check ones for aerial triangulation in experiments of section 4.

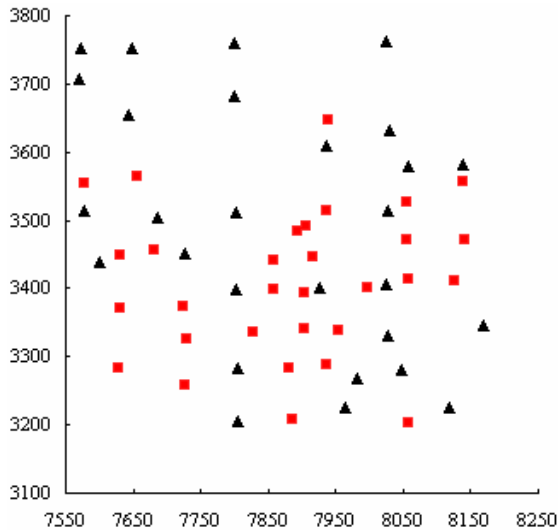


Figure 4. Distribution of control and check points

3. PHOTOGAMMETRIC PROCESSING OF LOW ALTITUDE IMAGE SEQUENCES

3.1 Image matching

Image matching is the prerequisite for aerial triangulation and 3D information extraction. It is also one of the cores of geometric processing. Camera orientations usually vary with time among adjacent images, because the posture of the stabilising platform is not so accurate. For example, 3 degrees variation in pitch and roll angle will result in about $\pm 5\%$ changes in forward and side overlap. In extreme circumstance, the real overlap between adjacent images will change 10% against the predefined overlap, i.e. may be 70% to 90% if the predefined forward overlap is 80%, or 20% to 40% if the predefined side overlap is 30%. Variation in yaw angle will also bring problems of overlap. As shown in figure 5, the above motioned deficiencies distinctly worsen the problem of image matching. So how to find some overall optimum conjugate points and thus estimate the orientation variation between stereo image pairs are the key technologies to match low altitude image sequences.

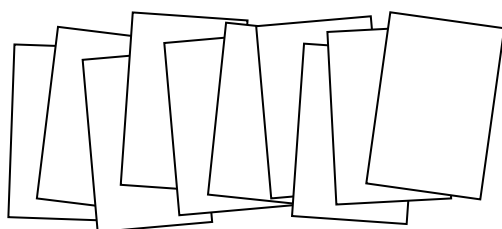


Figure 5. Sketch map of images acquired by low altitude remote sensing system in extreme circumstance

Image matching includes three steps, feature points extraction, overall matching and fine matching. Firstly, feature points are automatically extracted with Harris corner detector (Harris,

1988) from all images. In this process, each image is divided into regular grids with size of 90pixels* 90pixels. One feature point with maximum interested value that larger than a certain predefined threshold is extracted in each grid. For the camera Kodak Pro SLR with image format 4500pixels*3000pixels, at most 1650 feature points can be extracted from each image.

In the overall matching process, searching range of conjugate point in the right image for a certain feature point in the left image is usually 40% of the image format. That means if the predefined forward overlap is 70%, the searching range of conjugate point in the right image is from 50% to 90% in x-direction and from 80% to 120% in y-direction. As shown in figure 6, the black rectangle represents left image of a stereo, the purple rectangle represents the right image with 70% predefined forward overlap. Searching range is from 50% (blue rectangle in figure 6a) to 90% (dashed red rectangle in figure 6a) in x-direction, and from 80% (blue rectangle in figure 6b) to 120% (dashed red rectangle in figure 6b) in y-direction. Changes of yaw (κ) angle in the range of ± 15 degrees is also considered (blue and dashed red rectangle in figure 6c). This strategy ensures that images with large orientation change or containing large parallax objects such as tall buildings and high mountains can also be matched successfully. But caution that the larger the searching range, the more the mismatches. So only feature points with strong interested value in the left image are used to find overall conjugate ones in the right image. Once 5 or more overall optimum conjugate points are successfully matched, relative orientation can be performed to determine the overlaps and rotation angles between stereo pairs. Of course, gross mismatches should be detected and removed while calculating relative orientation parameters.

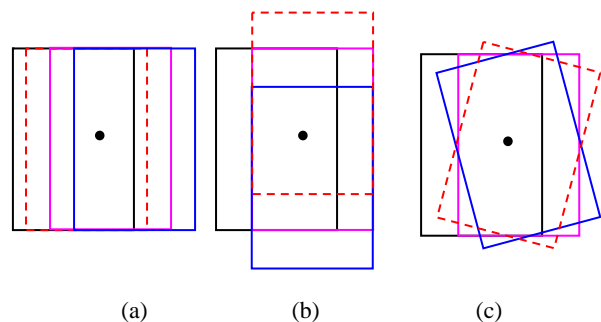


Figure 6. Searching range of conjugate point in the right image

Fine matching can be performed as long as relative orientation parameters are available. Pyramid strategy is always used for fine matching. This process is somewhat similar as traditional image matching. The overlap between adjacent stereo pair determined above can be used to predict the position of possible conjugate point for a certain feature point. Then precise least squares image matching is used to find the conjugate point in a local searching area around the predicted position along epipolar line determined by relative orientation parameters. After more conjugate points are matched, the relative orientation process is called to refine orientation parameters. Gross mismatches are detected and removed in relative orientation process. Then precise matching is again performed. Usually, matched points will be stable within three iterations. Note that for convenience of linking all stereo models automatically, matched image points in one stereo pair should transfer to the next stereo pair. This purpose can be realized by replacing feature point of left image with matched conjugate point in the same grid from the former stereo pair.

3.2 Relative orientation and model link

Relative orientation can be used to determine the orientation parameters of the right image when taken that of the left image as known. Orientation parameters of the first image are usually assumed as zero. At the same time, mismatches that do not obey the coplanarity condition used by relative orientation can also be founded and thus removed. In most cases, relative orientation is used in conjunction with image matching. There are usually significant lens distortions in images acquired by non-metric cameras. So lens distortion parameters calibrated in advance should be considered in relative orientation process.

All models in one strip can be automatically linked together by determine the baseline length with pass points that derived from image matching process. If a set of images include more than one strips, orientation parameters beside the first strip should be transformed through common points between adjacent strips. This work can be done by calculating seven parameters (three translations, three rotations and one scale) between two strips with model coordinates of common points.

3.3 Aerial Triangulation

There are inevitably discrepancies among camera parameters and model coordinates of conjugate points after model link. So free network bundle adjustment is performed to eliminate these discrepancies. Then absolute orientation parameters (usually seven parameters) can be easily calculated with model coordinates and world coordinates of ground control points. Initial values of unknowns in aerial triangulation can be obtained by absolute orientation process with results of free network adjustment.

Aerial triangulation with ground control points is the key of geometric precision analysis and prerequisite of 3D information extraction. Collinearity equation is still the basic mathematic model of aerial triangulation. Because the camera used for data acquisition is non-metric, interior parameters will change a little bit from time to time. The pre-calibrated interior parameters will not exactly the same as that of the truth of data acquisition. So self-calibration strategy is expected to be used in aerial triangulation. Furthermore, similar as traditional film based photogrammetry, there are also systematic errors in coordinates of images acquired by digital cameras (Cramer, 2007). High order correction polynomials like the 44 parameter Gruen model is introduced as unknowns in aerial triangulation. Self-calibration parameters of lens distortion are often closely correlated with additional systematic parameters. The two sets of parameters should not be unknowns at the same time in bundle adjustment.

Forward and side overlaps of low altitude image sequences are both higher than that of the traditional photogrammetry. A certain ground point usually has several corresponding image points. So the geometric model of low altitude image sequences is stronger than traditional photogrammetry. Another advantage is that the precision and reliability of aerial triangulation of low altitude image sequences will also increase since there are more redundant observations. So the precision of aerial triangulation will also superior to that of traditional photogrammetry.

4. EXPERIMENTS AND RESULTS

Experimental results of the proposed approaches will be discussed in this section. Low altitude image sequences and ground control points are used as sources of information.

Results of image matching, aerial triangulation and digital photogrammetric products generation such as DSM, DOM and DLG will be discussed in the following.

4.1 Image matching

There are about 600 to 800 successfully matched conjugate points in each image pair with the proposed approach of low altitude image matching. Figure 7 shows the matched conjugate points of one stereo pair. As can be seen, all conjugate points are randomly distributed in overlapped areas. These conjugate points are enough for aerial triangulation. They can also be used to analyze the forward and side overlaps or relative rotation angles between adjacent images. The mean forward overlaps between adjacent images are well fitted with the predefined 80%. The maximum forward overlap between adjacent image pairs is about 85%, and the minimum is about 75%. The maximum side overlap between images of adjacent strips is about 80%, and the minimum is about 70%. As compared with the predefined 80% forward overlap and 75% side overlap, maximum overlap variation is about 5% in both directions. The maximum orientation variation between adjacent images of the same strip is usually less than 5 degrees.



Figure 7. Matched conjugate points of a stereo pair

However, rotation angles between images that belong to different strips usually larger than that belong to same strip. As shown in figure 8, the rotation angle (κ) between two images of adjacent strips is about 9 degrees. Sometimes, this angle will be about 15 degrees. As can be seen in Figure 8, although the amount of conjugate points matched by the proposed algorithm is less than that in figure 7, almost all of them are exact conjugates. These conjugate points are vital for aerial triangulation because they link different strips together.



Figure 8. Matched conjugate points of images of adjacent strips

4.2 Aerial triangulation

The precision of terrestrial feature extraction is one of the key problems that the low altitude remote sensing system faces. It directly determines whether the low altitude remote sensing system can be used in practice. To fully evaluate the precision that the system can achieve, aerial triangulation with ground control points is performed in this section. Results of many bundle adjustment experiments show that taken lens distortion parameters as unknowns are not as effective as additional parameters. So only additional parameters are treated as unknowns in the following experiments.

4.2.1 Aerial triangulation with 80% forward and 75% side overlap image data

Image data of all 13 strips are used as sources of information in this section. There are totally 68534 ground points in the test data, and 28469 of them have at least 3 corresponding image points. The maximum image points corresponded to a ground points is 27, which is impossible in traditional photogrammetry. As shown in figure 4, 33 of the 64 ground points measured by total station are used as ground control points (GCPs), and the other 31 are used as check points for aerial triangulation. The aerial triangulation with 13 strips image data includes two experiments, the first with additional parameters as unknowns and the second without. All configuration parameters for aerial triangulation are exactly the same for the two experiments.

Unit weight root mean square (RMS) error of the first experiment is 0.0023mm, i.e. better than 0.3 pixels. Error statistics of GCPs and check points is shown in table 1. As can be seen, the RMS error of planar position and height for GCPs are both better than 0.02m. The RMS error of planar position for check points is also quite small, and the RMS error of height is a little bit larger than 0.02m, i.e. about 0.4 GSD. The maximum error of GCPs and check points are all smaller than 3 times of corresponding RMS error, which means that there is no gross error in control and check points. Because only 60% forward overlap and 30% side overlap is used by traditional photogrammetry, the height precision is usually around 1.0 to 1.5 GSD. So the achieved height precision of check points in this experiment is definitely superior to that of the traditional photogrammetry.

Item		RMS	Mean	Maximum
Control Points	X	0.015	0.003	0.043
	Y	0.013	-0.001	-0.030
	Z	0.018	0.002	-0.052
Check Points	X	0.011	-0.002	0.025
	Y	0.010	-0.004	-0.028
	Z	0.021	-0.004	-0.061

Table 1. Precision of aerial triangulation with additional parameters by 80% forward and 75% side overlap data (m)

The results of aerial triangulation without additional parameters are shown in table 2. Unit weight RMS error is also 0.0023mm. As can be seen, precision of planar position for GCPs and check points are similar with the first experiment, while the height precision is distinctly decreased. For example the height precision of check points is about 1.3 GSD, more than 3 times of the precision in the first experiment. The maximum error of check points is also 3 times of the first experiment. This result shows that additional systematic parameters are essential in aerial triangulation of images acquired by non-metric digital cameras.

Item		RMS	Mean	Maximum
Control Points	X	0.019	-0.003	-0.060
	Y	0.018	-0.006	-0.090
	Z	0.039	-0.012	-0.083
Check Points	X	0.008	-0.002	-0.018
	Y	0.014	-0.006	-0.051
	Z	0.065	0.026	0.186

Table 2. Precision of aerial triangulation without additional parameters by 80% forward and 75% side overlap data (m)

4.2.2 Aerial triangulation with 80% forward and 50% side overlap image data

To evaluate the relationship between height precision and side overlap, image data of odd strips (7 strips) of the 13 strips are used as input data for aerial triangulation. There are totally 46636 ground points in the test data, and 17596 of them have at least 3 corresponding image points. The maximum image points corresponded to a ground points is 14. GCPs and check points are the same as the experiments in section 4.2.1. The aerial triangulation with 7 strips data also includes two experiments, the first with additional parameters as unknowns and the second without. All configuration parameters for aerial triangulation are also exactly the same as that of section 4.2.1.

Unit weight RMS error of aerial triangulation with additional parameters is 0.0024mm. Error statistics of control and check points is shown in table 3. As can be seen, RMS errors of planar position for GCPs and check points are both better than 0.02m. RMS errors of height for GCPs and check points are about 0.03m, i.e. 0.6 GSD. When compared with the result in section 4.2.1, the height precision is apparently decreased.

The results of aerial triangulation without additional parameters are shown in table 4. Unit weight RMS error is also 0.0024mm. As can be seen, precision of planar position for GCPs and check points has decreased a little bit, while height precision is distinctly decreased. For example the height precision of check points is about 1.6 GSD, about 3 times of the precision with additional parameters. This result also verifies that additional parameters are essential in aerial triangulation.

Item		RMS	Mean	Maximum
Control Points	X	0.016	0.003	0.042
	Y	0.012	-0.001	0.033
	Z	0.029	0.004	-0.087
Check Points	X	0.016	0.004	0.029
	Y	0.011	-0.002	-0.027
	Z	0.027	0.001	-0.070

Table 3. Precision of aerial triangulation with additional parameters by 80% forward and 50% side overlap data (m)

Item		RMS	Mean	Maximum
Control Points	X	0.017	-0.001	0.058
	Y	0.020	-0.001	-0.067
	Z	0.068	-0.013	-0.235
Check Points	X	0.027	-0.006	-0.081
	Y	0.021	-0.011	-0.076
	Z	0.080	-0.014	-0.277

Table 4. Precision of aerial triangulation without additional parameters by 80% forward and 50% side overlap data (m)

As can be seen from the experimental results of aerial triangulation, when compared with the 0.05m GSD, height precision of about 0.4 and 0.6 GSD can be achieved by 75% and 50% side overlap non-metric image sequences respectively. Bundle adjustment with additional parameters can significantly improve the height precision. The achieved height precision is significantly higher than traditional aerial triangulation, and consists with the theoretical analysis in section 3.4.

4.3 Digital products generation

Once aerial triangulation is finished, DSM can be generated by dense image matching and forward intersection. Firstly, feature points are extracted every 11 by 11 pixels in each image. Then conjugate image points are found by multi-image matching algorithms under constraints of the matched image points for aerial triangulation and known camera parameters. Finally, corresponding ground coordinates of all conjugate points are obtained by multi-image forward intersection (Zhang, 2005a). These ground points can be used to generate Delaunay triangles, which is the common data structure to represent 3D terrain information.

DOM can be obtained by ortho rectification from image sequences with known camera parameters and the above obtained DSM. Note that mosaic lines of ortho image should not go through objects above the ground such as buildings. Color and illumination are inevitably different among images especially images of different strips acquired by digital cameras. So the generated ortho image has to be further processed by dodging or other color adjustment techniques. Figure 9 shows the generated ortho image after color adjustment. The precision of DOM can be checked by known ground features such as GCPs. Coordinates of GCPs can be interactively measured from ortho image and then compared with the world coordinates measured by total station. Precision of the generated ortho image is about 0.045m, i.e. comparable with GSD, as compared with the world coordinates.



Figure 9. DOM of the test area generated by image sequences

DLG is another type of digital photogrammetric productions. The aerial triangulated image sequences are also used to interactively produce DLG with commercial Digital Photogrammetric Workstation (DPW) Virtuoso. Figure 10 shows the stereoscopically measured outlines of buildings from all images in the test area. Coordinates of GCPs are also

measured by stereo environment and then compared with world coordinates. Both planar and height precision are better than 0.05m, which means that the proposed approaches and the image sequences acquired by the low altitude remote sensing system are qualified for the precision requirements of 1:500 scale mapping.

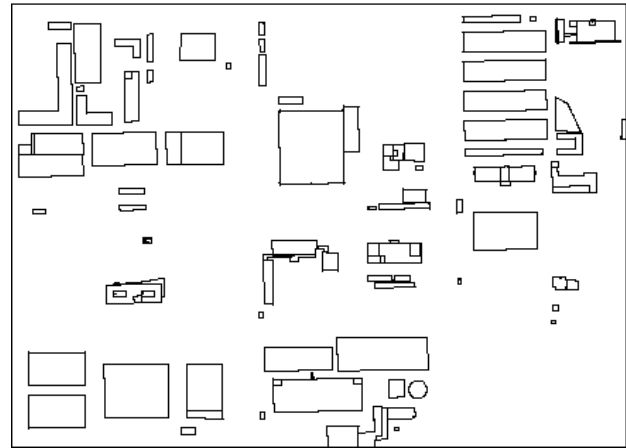


Figure 10. Measured outlines of buildings in the test area

5. CONCLUSIONS

The principles and technologies of photogrammetric processing of low altitude aerial images acquired by unmanned airship are discussed in this paper. The advantage of low altitude image sequences is that forward and side overlaps are both higher than that of traditional photogrammetry. Furthermore, geometric model of low altitude image sequences is also stronger. So the precision and reliability of aerial triangulation are higher since there are more redundant observations.

The proposed image matching approach can automatically find conjugate points from image pairs with different overlaps and large rotation angles. High order correction polynomials used in aerial triangulation can significantly improve the height precision. First results of image matching and aerial triangulation are very satisfying. Precision of ortho image and DLG also qualifies for the criteria of 1:500 scale mapping. Experimental results show that the proposed approaches and the developed low altitude remote sensing system are promising in large scale digital photogrammetry and precise 3D reconstruction areas.

Generating 3D models of buildings and other objects with low altitude image sequences will be the work in the near future. Introducing Global Positioning System (GPS) to measure coordinates of exposure points and thus decrease the number of required GCPs also need to be performed.

ACKNOWLEDGEMENT

This work is supported by National Natural Science Foundation of China with project number 40671157 and 40620130438, Program for New Century Excellent Talents in University with project number NCET-07-0645, Hi-Tech Research and Development Program of China with project number 2006AA12Z136 and National Key Technology Research and Development Program with project number 2006BAJ09B01.

REFERENCES

- Altan M. O., Celikoyan T. M., Kemper G., Toz G. , 2004. Balloon photogrammetry for cultural heritage. *The International Archives of the Photogrammetry, Remote Sensing and Spatial Information Sciences*, Istanbul, Turkey, Vol.35, Part B5, pp. 964-968.
- Bitelli G, Girelli V. A., Tini M. A., Vittuari L. , 2004. Low-height aerial imagery and digital photogrammetrical processing for archaeological mapping. *The International Archives of the Photogrammetry, Remote Sensing and Spatial Information Sciences*, Istanbul, Turkey, Vol.35, Part B5, pp. 498-503.
- Cramer, 2007. The EuroSDR performance test for digital aerial camera systems. *Photogrammetric Week 2007*, Wichmann, Heidelberg, pp. 89-106.
- Harris C G, Stephens M J, 1988. A combined corner and. edge detector. *Proceedings of Fourth Alvey Vision Conference*, Manchester, UK, pp. 147-151.
- Huang H. H., Lin S. Y, 2003. Digital photogrammetry using tethered balloon. *Journal of Photogrammetry and Remote Sensing of Taiwan*. 8(2), pp. 55-68.
- Karras G. E., Mavromati D., Madani M., et al, 1999. Digital orthophotography in archaeology with low-altitude non-metric images. *The International Archives of the Photogrammetry, Remote Sensing and Spatial Information Sciences*, Vol. 32 Part B5, pp. 8-11.
- Nogami, J., Phuon D., Kusanagi M., 2002. Field observation using flying platforms for remote sensing education. *23rd Asian Conference of Remote Sensing*, Kathmandu, Nepal, No.200.
- Sun J., Lin Z. J., Cui H. X., 2003. Low altitude remote sensing monitoring system based on UAVRS-II. *Remote Sensing Information*, 1(1), pp. 49-51.
- Zhang Y. J., Zhang Y, 2005a. Analysis of precision of relative orientation and forward intersection with high-overlap images. *Geomatics and Information Science of Wuhan University*, 30 (2), pp. 126-130.
- Zhang Y., Zhang Z., Zhang J., Wu J, 2005b. 3D building modeling with digital map, LIDAR data and video image sequences. *The Photogrammetric Record*, 20(111), pp. 285-302.

